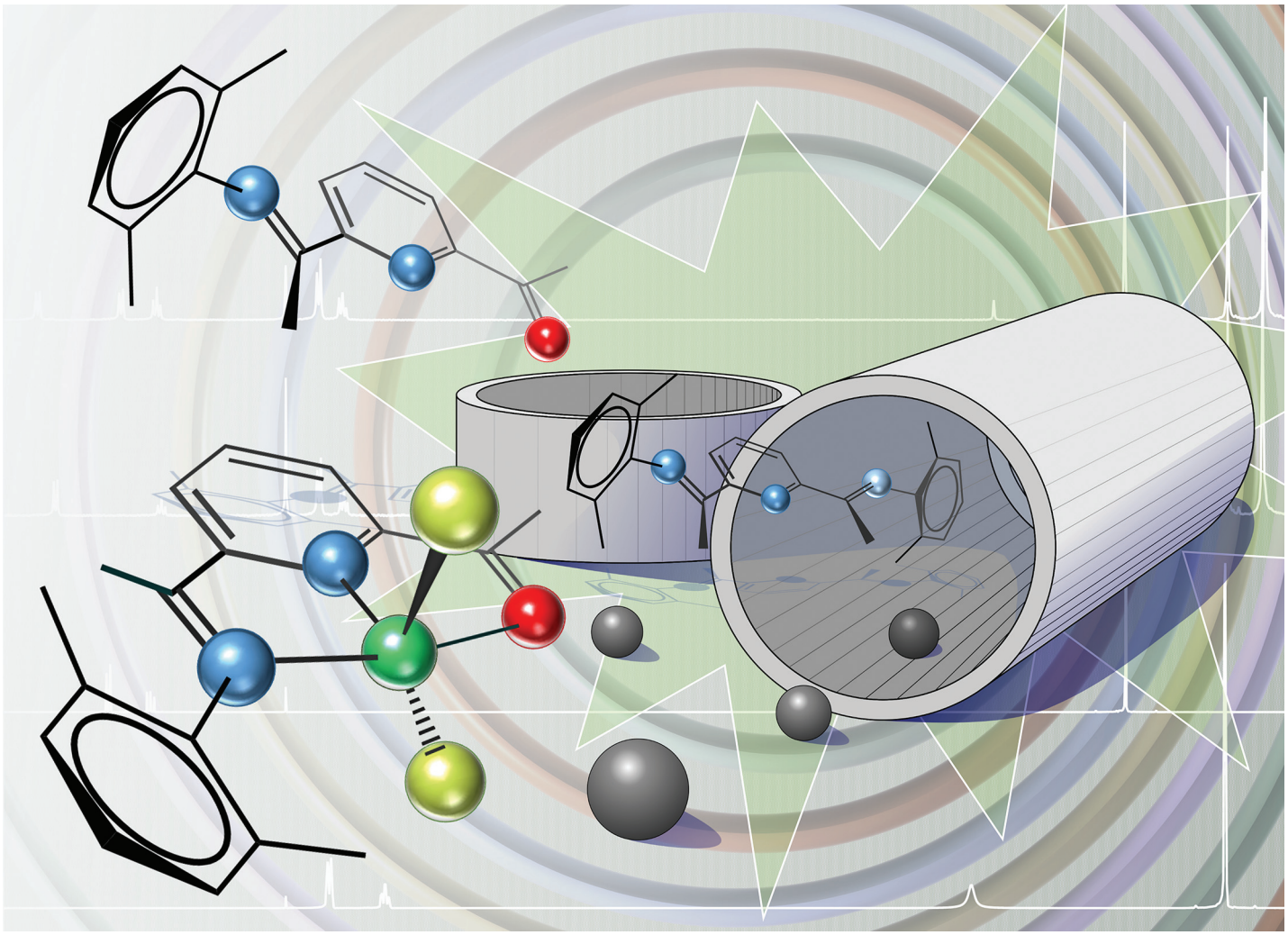

Showcasing research from the Jurca lab at the University of Central Florida.

Mechanochemical routes for the synthesis of acetyl- and bis-(imino)pyridine ligands and organometallics

Mechanochemical synthesis provides a facile and sustainable route to acetyl- and bis-(imino)pyridine pincer complexes, a ubiquitous ligand class for organometallic precatalysts. The approach is extended to the one-pot synthesis of acetyl(imino) pyridine-$CoCl_2$, where the ligand is formed *in-situ*.

As featured in:

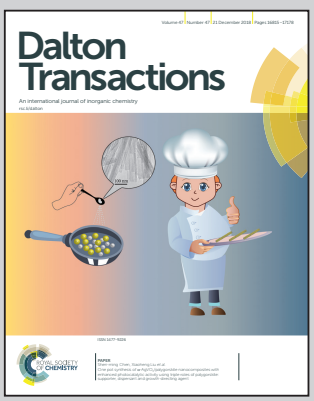

See Titel Jurca *et al.*, *Dalton Trans.*, 2018, **47**, 16876.

ROYAL SOCIETY OF CHEMISTRY

rsc.li/dalton

Registered charity number: 207890

Dalton Transactions

PAPER

View Article Online
View Journal | View Issue

Cite this: *Dalton Trans.*, 2018, **47**, 16876

Mechanochemical routes for the synthesis of acetyl- and bis-(imino)pyridine ligands and organometallics†

Thomas E. Shaw,[a] Lorianne R. Shultz,[a] Louiza R. Garayeva,[a] Richard G. Blair,[b] Bruce C. Noll[c] and Titel Jurca *[a]

Received 5th September 2018,
Accepted 12th October 2018

DOI: 10.1039/c8dt03608j

rsc.li/dalton

Organometallic precatalysts play a pivotal role in organic synthesis. However, their preparation often relies on multiple time, energy, and solvent intensive steps, including the synthesis of supporting organic ligand structures, and finally installation on the desired metal centres. We report the sustainable mechanochemical synthesis of acetyl- and bis-(imino)pyridine pincer complexes, a ubiquitous ligand class for organometallic precatalysts. The approach is extended to the one-pot synthesis of acetyl(imino)pyridine-$CoCl_2$, where the ligand is formed *in situ*.

Introduction

The advancement of modern molecular and macromolecular organic chemistry has been intimately linked with the development of organometallic precatalysts.[1] Although the use of catalysis is an important tool for sustainable synthesis, the majority of organometallic precatalysts are made by conventional, unsustainable routes which encompass multiple reaction steps, each with respective solvent and energy intensive workup procedures. Therefore, the development of more sustainable preparative routes to catalytically relevant organometallic species remains an important area of research.[2]

Over the past decade, mechanochemistry, conducted by milling or grinding, has emerged as a powerful tool for sustainable organic synthesis.[3,4] This has facilitated the development of numerous routes to value-added chemicals, and discovery of novel catalytic methodologies that are either solvent-economical, or solvent-free.[5] By contrast, sustainable mechanochemical routes towards organometallic complexes, or related organic ligand architectures have been greatly underdeveloped.[6] Nonetheless, in the past few years, landmark reports from the groups of Friščić,[7] Lamaty,[8] James,[9] Hanusa,[10] and others,[11] have emerged in this promising area.

We sought to contribute to this emerging field by developing sustainable mechanochemical routes to the pincer-type acetyl- and bis(imino)pyridine ligands. Although bis(imino)pyridines have been employed since the 1950s,[12,13] it wasn't until the mid-90s that they became a mainstay in organometallic chemistry as ligands for Co and Fe-based precatalysts for olefin polymerization.[14] Since then, bis(imino)pyridine, and to a lesser extent, related acetyl(imino)pyridine ligands have been employed broadly in coordination chemistry in support of both transition-metal and main-group compounds covering the majority of the periodic table.[14b,15] These complexes have been used in service of wide ranging applications, including precatalysts for polymerization,[16] alkene hydrogenation,[17] electrochemical hydrogen production,[18] as single molecule magnets,[19] and in studies for flow batteries.[20] While these ligands facilitate many downstream sustainable processes, their preparation is anything but green; conventional synthesis typically involves prolonged reflux in toluene or methanol (12–72 h) with subsequent solution-based workup (Scheme 1).[14b,21]

Herein, we report the facile and scalable mechanochemical synthesis of acetyl- (**3x**) and bis-(imino)pyridines (**4x**) with a

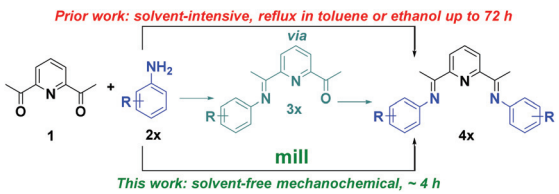

Scheme 1 Comparison of synthesis routes for bis(imino)pyridine ligands (**4x**), *via* acetyl(imino)pyridine intermediates (**3x**).

[a]*Department of Chemistry and the Energy Conversion and Propulsion Cluster, University of Central Florida, 4353 Scorpius Street, Orlando, FL, 32816, USA. E-mail: Titel.Jurca@ucf.edu*
[b]*Florida Space Institute, University of Central Florida, 12354 Research Parkway, Suite 214, Orlando, FL, 32826, USA*
[c]*Bruker AXS Inc., 5465 East Cheryl Parkway, Madison, WI, 53711, USA*

†Electronic supplementary information (ESI) available: Materials, methods, optimization and spectroscopic data. CCDC 1861815. For ESI and crystallographic data in CIF or other electronic format see DOI: 10.1039/c8dt03608j

range of substitution patterns and functionalities (Scheme 1), utilizing no solvents for synthesis,[22] and only minimal solvents for purification. We extended this methodology to the synthesis of a Co-based organometallic complex; a one-pot, *one-step* process, which yields acetyl(imino)pyridine-cobalt(II)chloride in high yield (86%) and purity. To our knowledge, this is the first report of a mechanochemical one-pot, *one-step* process where both ligand and organometallic species are formed *in situ* from their respective precursors.[23]

Results and discussion

To delineate the conditions necessary for the mechanochemical synthesis of bis(imino)pyridines, we conducted a series of experiments varying additives, grinding auxiliaries, size and number of balls, and time for the reaction of **1** and **2a** (a common aniline for (imino)pyridine ligands) (Scheme 2). All reactions were conducted in a 316 stainless steel vessel with an internal volume of 4.6 cm^3 on a SPEX 5100 Mixer/Mill® ball mill (50 Hz).[24] Stainless steel balls (440c) were used as the milling media. Reactions were monitored by ^{1}H NMR (Fig. S1†). Notably, catalytic amounts of *p*-toluenesulfonic acid monohydrate (TsOH) are required for reactivity. $MgSO_4$ serves as desiccant to drive the condensation reaction, increasing the overall rate. Its role as a grinding auxiliary is minimal, as replacement with Celite® 545 results in identical yields to reactions with only TsOH. The combination of (4) 3.175 mm balls slightly outperformed reactions run with (1) 3.175 mm or (1) 6.35 mm ball. The addition of methanol to facilitate liquid assisted grinding (LAG) as **2a** (oil) is consumed appeared to have no effect on the rate. The following parameters resulted in the highest yield over a 4 hour period (17% **3a**, 80% **4a**): **1** = 1.2 mmol, **2a** = 3.8 mmol, $MgSO_4$ = 200 mg, TsOH = 7 mg, and (4) 3.175 mm balls for a free volume in the vial of ~3.75 cm^3.[24]

Utilizing this protocol, reaction progress, and temperature (*measured in vessel immediately after removal from mill*) as a function of time were monitored over 4 h (separate reactions). The reactions proceed stepwise with initial formation of **3a**, followed by conversion to **4a**, with no observable by-products (Fig. 1 and S3†). While the temperatures recorded are not fully representative of *in situ* reaction conditions, they reveal that the average temperature of the bulk remains low (<45 °C) (Table S1†), which likely helps to mitigate by-product formation.

By calculating concentration as the moles of compound per volume of free space in the reaction vessel, it is possible to perform kinetic analysis on the reaction progress.[25] Both the final product and precursor followed simple kinetics with reactant **1a** consumption occurring as a first order process with a rate of 0.014 (±0.0012) min^{-1} and the production of **4a** as a pseudo-zeroth order process with a rate of 8.8 (±0.7) × 10^{-4} mol L^{-1} min^{-1}. The formation of **3a** is much faster than that of **4a** from **3a**. In essence, there is an excess of **3a** leading to the observed pseudo-zeroth order kinetics (Fig. S4†).

With optimized conditions in hand, we expanded the scope to 8 other anilines (**2b–i**) bearing a range of substitution patterns and functionalities (Scheme 3). With the exception of **2i**, all reactions produced a combination of both **3x** and **4x** with no additional by-products observed (***x*** = ***a–i***). Isolated yields were calculated after drying of crystalline precipitates. Compounds **3a** and **3b** were readily isolated by treating the reaction crude with minimal methanol and passing through a 0.2 μm PTFE filter. However, **3c** and **3d** could only be isolated

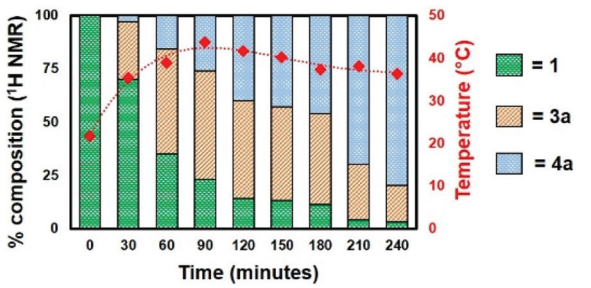

Fig. 1 (*left*) % composition for the synthesis of **3a** and **4a** at 30 min intervals assessed by ^{1}H NMR. (*right*) peak temperatures.

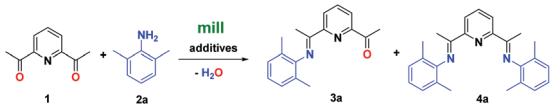

Scheme 2 Formula for the mechanochemical synthesis of **3a** and **4a**.

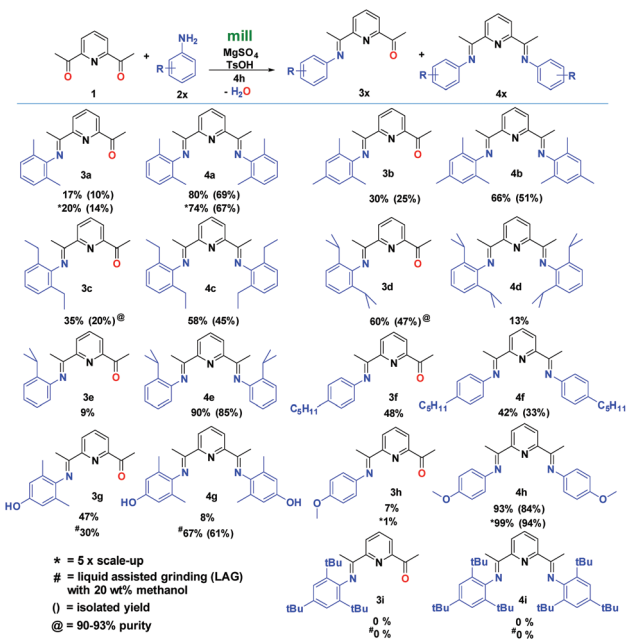

Scheme 3 Mechanochemical synthesis of **3x** and **4x**. **1** = 1.2 mmol, **2x** = 3.8 mmol, $MgSO_4$ = 200 mg, TsOH = 7 mg, (4) 3.175 mm steel balls, steel vessel, SPEX 5100 mill. * = 5× scale-up, (2) 11.2 mm WC balls, SPEX 55 mL WC vial, SPEX 8000 mill.

in 90% and 93% purity (^{1}H NMR) with small amounts of respective co-precipitates **4c** and **4d** present. Species **3f–h** were readily observed by ^{1}H NMR but could not be isolated with reasonable purity by this method. Treating the same reaction crude with pentane afforded rapid precipitation of **4a–c,e,f**, whereas **4g** and **4h** required minimal dichloromethane (or THF for **4h**) due to poor solubility in pentane. In general, isolated yields of selectively precipitated species were good (~57–75% of NMR yield for **3x** and 77–90% for **4x**). Reactions with **2a** and **2h** were scaled up 5 fold utilizing (2) 11.2 mm tungsten carbide (WC) balls, a SPEX 55 mL WC vial (model 8004) giving a free volume of ~30 cm^3. Milling was performed on a SPEX 8000M mill (18 Hz) for a reaction time of 4 h (continuous). NMR yields were slightly lower for **2a** (74% *vs.* 80% for **4a**), however near quantitative conversion was achieved with **2h**.

The as-tested reaction time of 4 h serves as a benchmark to compare the reactivity of various anilines. Based on the optimization studies conducted for **2a** (*vide supra*), prolonged reaction times should furnish higher yields across the range (**2b–h**). Anilines **2a–f** are oils which facilitated LAG, whereas **2g–i** were solids; **2h** has an mp of 56–59 °C, which may have been attained under reaction conditions. Nonetheless, **2h** resulted in complete conversion of **1**, the highest conversion to disubstituted species (93% **4h**), and the highest isolated yield (84%). Aniline **2g** resulted in 55% conversion of **1** to give a predominant yield of **3g** (47%) with minimal **4g** (7%). This was dramatically improved by the addition of 20 wt% methanol (*slurry*), facilitating 97% conversion of **1** with a predominant distribution of 67% **4g** and 30% **3g**. Aniline **2i** did not react under neat or slurry conditions, likely due to the steric bulk imposed by the *ortho-tert*butyl groups flanking the NH_2.

In general, conversion of **1** (*sans* MeOH) corresponds well to aniline molecular weight (Fig. S15†). Higher MW precursors results in a lower ball to reagent ratio. This lowered ratio also corresponds to a smaller free volume, lower media velocities, and lower impact forces. This broadly led to lower conversions of **1** as reagent weight increased. Steric factors also appear to play a role, particularly for the overall yield of **4x**. While reactions with **2a** and **2h** have very similar ball to reagent ratios of 0.594 and 0.577 respectively, **2h** (no *ortho* substituents) facilitated 93% conversion to **4h** *vs.* 80% for **2a** (two *ortho* methyl groups) to **4a**. Similarly, **2b** and **2e** have identical molecular weights, and ball to reagent ratios of 0.548, however, **2e** only features a single *ortho* substituent. The result was a 90% conversion to **4e** *vs.* only 66% for **4b**. Aniline **2f** bears no *ortho* substituents and should feature no steric impediment, however, conversion of **1** was only 90%, with **3f** and **4f** at 48% and 42%, consistent with a lower ball to reagent ratio (0.491).

To assess the advantages of our method, we compare the parameters of our process for the synthesis of **4a** and **4b** to the common solution based protocols from the literature.[14a,26] The parameters evaluated are (i) reaction solvent per grams of isolated yield, (ii) workup solvent per grams of isolated yield, (iii) reaction time (h), and (iv) % isolated yield (Fig. 2 and Table S2†). While all literature protocols report the amount of solvent used for reaction, the total amount of solvent for subsequent workup remains undisclosed; exclusive of **3g** and **4g**, our reaction process is entirely solvent free. Additionally, most protocols report reaction time as an overnight reflux. Since this is not strictly quantified, a time of 12 h was tentatively assigned; notably, the mechanochemical processes reported herein operate on a timer and are stopped at 4 h. As is evident, our streamlined process affords competitive yields, which can be further enhanced through prolonged reaction time (Fig. 1). The noted reaction time of 4 h represents a dramatic improvement over conventional synthesis. This has broader implications on power consumption, as extended reflux periods require more energy input than driving the small electric motor of a ball mill for 4 h.[27] Moreover, the workup protocol reported can facilitate the isolation of both **3x** and **4x**, giving higher return on solvent, time and energy expenditure compared to conventional literature processes.

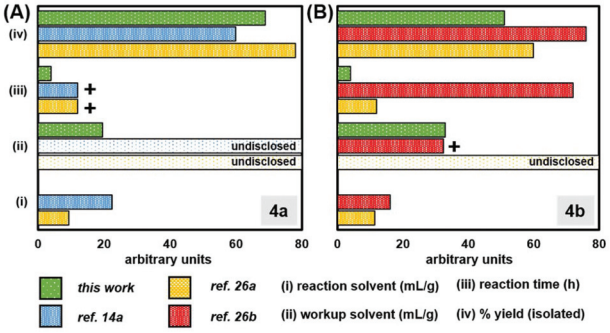

Fig. 2 Comparison of experimental protocols for the synthesis of **4a** (A) and **4b** (B). *Note: "+" indicates a higher partially undisclosed amount*.

An attractive feature of pincer-type ligands is the ability to introduce multiple different functional groups,[28] rendering the ligand architecture asymmetric. This can have profound implications for tailoring catalyst reactivity and selectivity. The benefit of readily isolable mono-substituted **3x**, is their potential application in the synthesis of unsymmetrically substituted bis(imino)pyridines. Mechanochemical reaction of **3a** with **2b** under similar conditions as detailed in Scheme 3 results in the formation of **4ab** (Scheme 4). As expected, a similar product is obtained from the reaction of **3b** with **2a**. Isolated yields after workup were good (71% and 62% respectively). The structure of **4ab** was confirmed by single crystal X-ray diffraction (Scheme 4, *inset*).

Encouraged by our findings on the synthesis of **3x** and **4x**, we sought to expand this protocol to the one-pot synthesis of related Co-based organometallic complexes.[14,15,16a,17] To set a benchmark, mechanochemically synthesized **4a** was reacted with dehydrated $CoCl_2$ under conventional Schlenk conditions, with either THF or toluene as solvent, to yield literature compound **5** (Scheme 5i). Utilizing a similar mechanochemical protocol as the 5× scale up reaction (*vide supra*), we attempted a *one-step*, one-pot synthesis of **5** (Scheme 5ii). However, this resulted in the isolation of **6** in high yield (86%), and high purity.

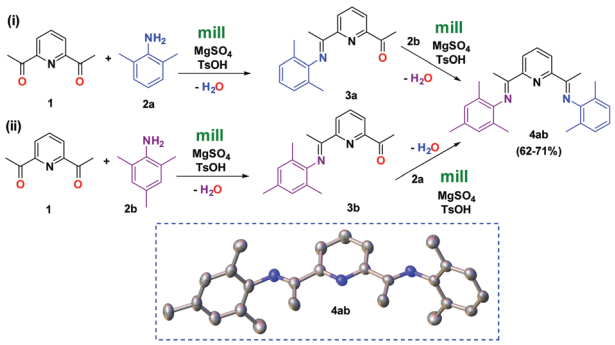

Scheme 4 Synthesis of unsymmetrically substituted **4ab**. *Inset*: structure of **4ab** with thermal ellipsoids drawn at the 50% probability level. For bond lengths [Å] and angles [°] see Tables S4 and S5.†

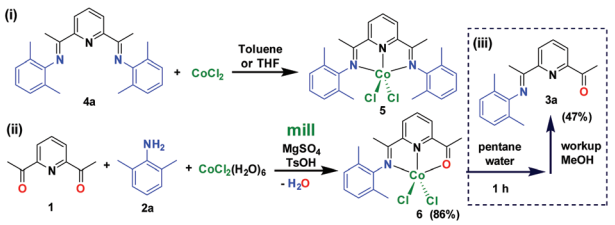

Scheme 5 (i) Conventional synthesis of **5**; (ii) mechanochemical reaction of **1** and **2a** and $CoCl_2(H_2O)_6$ for 4 h leading to **6**; (iii) reaction of **6** with 1 : 1 water : pentane leading to isolation of **3a**.

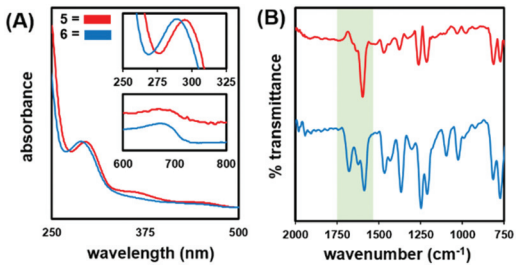

Fig. 3 (A) UV-Vis in DCM and (B) FTIR spectra of **5**, and **6**.

Both **5** and **6** are green solids exhibiting similar appearance and solution behaviour; they were characterized by UV-Vis and FTIR spectroscopy (Fig. 3). The results were consistent with prior reports. By UV-vis, **5** features a broad peak at 296 (ligand π–π*), and two lower intensity very broad peaks at 360–380 and 440–470 nm (MLCT); **6** features a similar broad absorption at 289 (π–π*) and a lower intensity one at 430–470 nm (MLCT). Both **5** and **6** display very low intensity absorptions at 650–700 nm (likely d–d).[14c] FTIR of **6** features characteristic peaks at 1679 cm^{-1} ($\nu_{C=O}$) and 1598 cm^{-1} ($\nu_{C=N}$); the latter is also present for **5**. We tentatively attribute the formation of **6** to a combination of (a) rapid chelation of intermediate **3a** to $CoCl_2$ (b) the apparent high stability of **6** in the reaction system, and (c) the potential hydrolysis of any **5** present to regenerate **6** (Scheme S1†).[29]

To our knowledge, this is the first report of a mechanochemical *one-step*, one-pot, multicomponent synthesis of an organometallic species where the ligand itself is formed *in situ*.[22] Comparatively, the two-step (ligand then organometallic) solution-based preparation of **6** has a global yield of 26%.[16a] Finally, treatment of **6** with a 1 : 1 mixture of water and pentane, then extraction of the organic phase and recrystallization from methanol resulted in the isolation of **3a** in moderate yields (47%, Scheme 5iii). Further optimization of this approach may provide a facile route to acetyl(imino)pyridines **3x** which would otherwise be difficult to isolate by other preparatory routes, thereby creating a broader library of precursors for unsymmetrical bis(imino)pyridines.

Conclusions

The complete removal of solvent from, or replacement of toxic solvents with environmentally friendly alternatives for organic synthesis remains an ongoing challenge. The work presented herein makes significant strides to removing solvent from the reaction process, and developing streamlined workup protocols which limit overall solvent use for the synthesis of a ubiquitous class of ligands. Notably, the process is simple, and very time-efficient, with comparable yields to conventional solution-based processes. The corollary of dramatically reduced reaction times (4 h *vs.* 12–72 h) is a savings in overall energy input, and an increase in overall efficiency. Application of the methodology to the one-pot synthesis of Co-based organometallics resulted in selective formation of acetyl(imino)pyridine cobalt(II) species **6**, with dramatically improved yield compared to conventional synthesis (86% *vs.* 26%). Understanding the mechanism leading to this product selectivity, and expansion of the variety of both ligand functionality and metal centre is the focus of ongoing investigation. These initial findings are promising for the future development of solvent-free on-demand synthetic processes for imino-pyridine based organometallic precatalysts.

Experimental

General methods

Unless otherwise stated, all reactions were carried out under air, at ambient temperature (21–23 °C, 40–51% relative humidity). Cobalt(II)chloride hexahydrate, diacetylpyridine (**1**) and anilines **2a–i** were purchased from TCI America, *p*-toluenesulfonic acid monohydrate (TsOH), chloroform-*d* ($CDCl_3$) and acetone-*d*6 ($(CD_3)_2CO$) were purchased from Acros Organics, and $MgSO_4$ was purchased from Strem Chemicals, and used as received. Solvents were purchased from Fisher Scientific and used without any further purification. Mechanochemical synthesis was conducted with a SPEX® 5100 high-energy ball mill for small/test scale reactions, and with a SPEX® 8000M high-energy ball mill for scaled-up reactions. Small scale reactions were conducted in a 316 stainless steel vial with an internal

volume of 4.6 cm^3 used by Mack *et al.* in previous work,[24] while scaled-up reactions were conducted in a SPEX®® 55 mL tungsten carbide vessel (model 8004). Small scale organic reaction mixtures were filtered through Fisher Scientific basix™ 0.2 μm PTFE syringe filters, while scaled-up reactions were filtered through VWR 494 filter paper. Organometallic reactions were filtered through fine porosity glass frits. {2,6-Bis{1-[(2,6-dimethylphenyl)imino]ethyl}pyridine}$CoCl_2$ (**5**) (Scheme 5, rxn i) was synthesized utilizing standard literature Schlenk protocol under N_2 atmosphere and with anhydrous solvents (THF or toluene), and dehydrated $CoCl_2$.[26a,30] As expected, both solvents led to identical products. All NMR spectra were acquired on a Bruker Avance III 400 MHz spectrometer, and processed with Mestrelab's MestReNova 10.0 software. Spectra were referenced to either residual $CHCl_3$ (^{1}H δ 7.26, ^{13}C δ 77.36) or ($(CH_3)_2CO$) (^{1}H δ 2.09, ^{13}C δ 30.60) for the respective deuterated solvent used.[31] FTIR Spectra were measured on a Bruker Vertex 70 with Helios ATR attachment. UV-Vis Spectra were collected on an Agilent Cary 60 spectrophotometer utilizing 1 cm quartz cuvettes purchased from Spectrocell Inc. Mass spectra were acquired on a Bruker EVOQ Qube® Triple Quad using electrospray ionization (ESI). Samples were prepared by serial dilutions to afford 2 ppm concentrations in 1 mL of methanol : water (51 : 49). Elemental analysis (C,H,N) was conducted by Galbraith Laboratories, Inc., Knoxville, TN USA.

Optimization experiments

In a steel vial, diacetylpyridine **1** [0.00184 mol (300 mg) for Fig. S2,† entries 1–14, 0.0012 mol (200 mg) for entry 15], was mixed with 0.0038 mol (455 mg) 2,6-dimethylaniline **2a**. Combinations of additives, grinding auxiliaries, and 440c stainless steel balls, as defined in Fig. S2† were added (entries 1–15). The reaction vessel was sealed, and placed on a SPEX® 5100 mill and allowed to react for the denoted durations. When complete, a sample of the powder/slurry was taken, dissolved in ~0.8 mL $CDCl_3$, and passed through a 0.2 μm PTFE syringe filter. The sample was measured by ^{1}H NMR spectroscopy, and the % composition was determined by the integration of the well-resolved pyridine *meta*-CH peaks (Fig. S1†). Notably, entries 2, 4, 8, 10, and 13 show broader peaks, which is due to presence of H_2O in the system as a result of no $MgSO_4$ additive to act as desiccant.

Timed reactions

In a steel vial, diacetylpyridine **1** 0.0012 mol (200 mg) was mixed with 0.0038 mol (455 mg) 2,6-dimethylaniline **2a**, 7 mg of *p*-toluenesulfonic acid monohydrate (TsOH), and 200 mg $MgSO_4$ with (4) 3.175 mm 440c stainless steel balls. The reaction vessel was sealed, and placed on a SPEX® 5100 mill and allowed to react for the denoted durations (Fig. S3,† 0–240 min at 30 min intervals). When complete, the temperature was measured in vessel immediately after removal from mill, and a sample of the powder/slurry was taken, dissolved in ~0.8 mL $CDCl_3$, and passed through a 0.2 μm PTFE syringe filter. The sample was measured by ^{1}H NMR spectroscopy, and the % composition was determined by the integration of the well-resolved pyridine *meta*-CH peaks (Fig. S1†). The corresponding conversions and temperatures are denoted in Table S1.† Notably, the temperature peaks and begins to decrease after 90 min, this is likely due to the different heat capacity of the mixture as the aniline oil is being consumed.

General procedure for the mechanochemical reaction of 1 with 2a–i

Unless otherwise specified, the following protocol was utilized: in a steel vial, diacetylpyridine **1** 0.0012 mol (200 mg) was mixed with 0.0038 mol of aniline **2x**, 7 mg of *p*-toluenesulfonic acid monohydrate (TsOH), and 200 mg $MgSO_4$ with (4) 3.175 mm 440c stainless steel balls. The reaction vessel was sealed, and placed on a SPEX® 5100 mill and allowed to react for 4 h. When complete a small aliquot of the slurry or powder was taken and measured by ^{1}H NMR spectroscopy, and the % composition was determined by the integration of the well-resolved pyridine *meta*-CH peaks (Fig. S1†). In general (*except for **3g**, and **3h***) the crude product was washed with 2 mL methanol and filtered through a 0.2 μm PTFE filter and held in a −24 °C freezer to crystallize the acetyl(imino)pyridine product **3x** (only for **2a–d**), while several passes with pentane (2 × 2 mL) followed by similar treatment afforded the bis(imino)pyridine product **4x** (only for **2a–c,e–h**). Isolated **4x** was further washed with 2 mL of cold methanol to remove any remaining **3x**. All reactions were reproducible within similar yields and product distributions. *Fig. S5–S13† detail the crude and isolated product ^{1}H and ^{13}C NMRs with tentatively assigned shifts based on prior literature reports, and expected splitting and integration.*

2-Acetyl-6-{1-[(2,6-dimethylphenyl)imino]ethyl}pyridine (3a). ^{1}H NMR (400 MHz, $CDCl_3$; δ, ppm) 8.58 (d, 1H, py_m–H), 8.14 (d, 1H, py_m–H), 7.95 (t, 1H, py_p–H), 7.09 (d, 2H, Ph_m–H), 6.96 (t, 1H, Ph_p–H), 2.79 (s, 3H, O=C(CH_3)), 2.22 (s, 3H, N=C(CH_3)), 2.04 (s, 6H, Ph–CH_3).[32] MS (ESI): *m*/*z* 267.1 $[M + H]^+$. ***2,6-Bis{1-[(2,6-dimethylphenyl)imino]ethyl}pyridine (4a)*:** ^{1}H NMR (400 MHz, $CDCl_3$; δ, ppm) 8.49 (d, 2H, py_m–H), 7.92 (t, 1H, py_p–H), 7.08 (d, 4H, Ph_m–H), 6.95 (t, 2H, Ph_p–H), 2.24 (s, 6H, N=C(CH_3)), 2.06 (s, 12H, Ph–CH_3). ^{13}C{^{1}H} NMR (100 MHz, $CDCl_3$; δ, ppm) 167.2 (C_q), 155.1 (C_q), 148.6 (C_q), 136.9 (C_q), 127.9 (Ar–CH), 125.5 (Ar–CH), 123.1 (Ar–CH), 122.2 (Ar–CH), 18.0 (Ar–CH_3), 16.5 (N=C(CH_3)).[32] (See Fig. S5†) MS (ESI): *m*/*z* 370.2 $[M + H]^+$. *Note: workup for **3a**/**4a** was optimized to 1 mL MeOH, 2 × 2 mL pentane, followed by 1 mL MeOH wash.*

2-Acetyl-6-{1-[(2,4,6-trimethylphenyl)imino]ethyl}pyridine (3b). ^{1}H NMR (400 MHz, $CDCl_3$; δ, ppm) 8.56 (d, 1H, py_m–H), 8.13 (d, 1H, py_m–H), 7.93 (t, 1H, py_p–H), 6.90 (s, 2H, Ph_m–H), 2.79 (s, 3H, O=C(CH_3)), 2.30 (s, 3H, Ph_p–CH_3), 2.23 (s, 3H, N=C(CH_3)), 2.00 (s, 6H, Ph_o–CH_3).[33] ***2,6-Bis{1-[(2,4,6-trimethylphenyl)imino]ethyl}pyridine (4b)*:** ^{1}H NMR (400 MHz, $CDCl_3$; δ, ppm) 8.48 (d, 2H, py_m–H), 7.91 (t, 1H, py_p–H), 6.90 (s, 4H, Ph_m–H), 2.30 (s, 6H, N=C(CH_3)), 2.24 (s, 6H, Ph_p–CH_3), 2.02 (s, 12H, Ph_o–CH_3). ^{13}C{^{1}H} NMR (100 MHz, $CDCl_3$; δ, ppm) 167.4 (C_q), 155.2 (C_q), 146.3 (C_q), 136.8 (C_q), 132.2 (C_q), 128.6 (Ar–CH), 125.3 (Ar–CH), 122.2 (Ar–CH), 20.8 (Ph_p–CH_3),

17.9 (Ph_o–$\mathbf{C}H_3$), 16.4 (N=C($\mathbf{C}H_3$)).[26a] (See Fig. S6†) MS (ESI): *m*/*z* 398.2 $[M + H]^+$.

2-Acetyl-6-{1-[(2,6-diethylphenyl)imino]ethyl}pyridine (3c). ^{1}H NMR (400 MHz, $CDCl_3$; *δ*, ppm) 8.57 (d, 1H, py_m–H), 8.14 (d, 1H, py_m–H), 7.95 (t, 1H, py_p–H), 7.13 (d, 2H, Ph_m–H), 7.05 (t, 1H, Ph_p–H), 2.79 (s, 3H, O=C(CH_3)), 2.37 (m, 4H, CH_2), 2.25 (s, 3H, N=C(CH_3)), 1.14 (t, 6H, CH_3). ***2,6-Bis{1-[(2,6-diethylphenyl)imino]ethyl}pyridine (4c)*:** ^{1}H NMR (400 MHz, $CDCl_3$; *δ*, ppm) 8.48 (d, 2H, py_m–H), 7.93 (t, 1H, py_p–H), 7.13 (d, 4H, Ph_m–H), 7.04 (t, 2H, Ph_p–H), 2.40 (m, 8H, CH_2), 2.26 (s, 6H, N=C(CH_3)), 1.15 (t, 12H, CH_3). $^{13}C\{^1H\}$ NMR (100 MHz, $CDCl_3$; *δ*, ppm) 166.9 (C_q), 155.1 (C_q), 147.8 (C_q), 136.9 (C_q), 131.2 (Ar–CH), 125.9 (Ar–CH), 123.3 (Ar–CH), 122.2 (Ar–CH), 24.6 (Ar–$\mathbf{C}H_2$–CH_3), 16.8 (N=C($\mathbf{C}H_3$)), 13.8 (Ar–CH_2–$\mathbf{C}H_3$).[34] (See Fig. S7†) MS (ESI): *m*/*z* 426.3 $[M + H]^+$.

2-Acetyl-6-{1-[(2,6-diisopropylphenyl)imino]ethyl}pyridine (3d). ^{1}H NMR (400 MHz, $CDCl_3$; *δ*, ppm) 8.57 (d, 1H, py_m–H), 8.15 (d, 1H, py_m–H), 7.96 (t, 1H, py_p–H), 7.19 (d, 2H, Ph_m–H), 7.12 (t, 1H, Ph_p–H), 2.80 (s, 3H, O=C(CH_3)), 2.73 (m, 2H, ^{i}Pr–CH), 2.27 (s, 3H, N=C(CH_3)), 1.16 (brm, 12H, ^{i}Pr–CH_3).[35] MS (ESI): *m*/*z* 323.2 $[M + H]^+$. ***2,6-Bis{1-[(2,6-diisopropylphenyl)imino]ethyl}pyridine (4d)*:** the following peaks could be clearly distinguished by ^{1}H NMR (400 MHz, $CDCl_3$; *δ*, ppm) 8.50 (d, 2H, py_m–H), 2.28 (s, 6H, N=C(CH_3)), 1.28 (d, 6H, ^{i}Pr–CH_3). The remainder overlap with those of **3d**.[36] (See Fig. S8†).

2-Acetyl-6-{1-[(2-isopropylphenyl)imino]ethyl}pyridine (3e). The following peaks could be clearly distinguished by ^{1}H NMR (400 MHz, $CDCl_3$; *δ*, ppm) 8.56 (d, 1H, py_m–H), 8.16 (d, 1H, py_m–H), 7.95 (t, 1H, py_p–H), 2.84 (s, 3H, O=C(CH_3)), 2.44 (s, 3H, N=C(CH_3)), 1.24 (d, 6H, CH_3).[35] ***2,6-Bis{1-[(2-isopropylphenyl)imino]ethyl}pyridine (4e)*:** ^{1}H NMR (400 MHz, $CDCl_3$; *δ*, ppm) 8.41 (d, 2H, py_m–H), 7.90 (t, 1H, py_p–H), 7.33 (d, 2H, Ph_o–H), 7.20 (t, 2H, Ph_m–H), 7.12 (t, 2H, Ph_p–H), 6.65 (d, 2H, Ph_m–H), 3.02 (m, 2H, ^{i}Pr–CH), 2.39 (s, 6H, N=C(CH_3)), 1.20 (brd, 12H, CH_3). $^{13}C\{^1H\}$ NMR (100 MHz, $CDCl_3$; *δ*, ppm) 166.5 (C_q), 155.5 (C_q), 148.7 (C_q), 138.2 (C_q), 136.8 (Ar–CH), 126.2 (Ar–CH), 125.7 (Ar–CH), 124.0 (Ar–CH), 122.2 (Ar–CH), 118.4 (Ar–CH), 28.5 (^{i}Pr–$\mathbf{C}$H), 22.9 (Ar–CH-($\mathbf{C}H_3$)$_2$), 16.5 (N=C($\mathbf{C}H_3$)).[34,37] (See Fig. S9†) MS (ESI): *m*/*z* 398.2 $[M + H]^+$.

2-Acetyl-6-{1-[(4-amylphenyl)imino]ethyl}pyridine (3f). In the crude, the following peaks could be distinguished by ^{1}H NMR (400 MHz, $CDCl_3$; *δ*, ppm) 8.49 (d, 1H, py_m–H), 8.12 (d, 1H, py_m–H), 2.80 (s, 3H, O=C(CH_3)). ***2,6-Bis{1-[(4-amylphenyl)imino]ethyl}pyridine (4f)*:** ^{1}H NMR (400 MHz, $CDCl_3$; *δ*, ppm) 8.34 (d, 2H, py_m–H), 7.86 (t, 1H, py_p–H), 7.19 (d, 4H, Ph_m–H), 6.78 (d, 4H, Ph_o–H), 2.62 (t, 4H, Ph–$\mathbf{C}H_2$-(CH_2)$_3$$CH_3$), 2.42 (s, 6H, N=C($CH_3$)), 1.64 (m, 4H, Ph–$CH_2$-($\mathbf{C}H_2$)$_3$$CH_3$), 1.35 (brm, 8H, Ph–$CH_2$-($\mathbf{C}H_2$)$_3$$CH_3$), 0.91 (brt, 12H, Ph–$CH_2$-($CH_2$)$_3$$\mathbf{C}H_3$). *Due to fluxionality in solution/multiple orientations of the imino-aryl/alkyl groups, a higher number of peaks in the ^{13}C are observed than would be expected for a symmetrical ligand*: $^{13}C\{^1H\}$ NMR (100 MHz, $CDCl_3$; *δ*, ppm) 166.6 (**C**=N), 156.2 (C_{Aryl}), 152.7 (C_{Aryl}), 152.4 (C_{Aryl}), 148.6 (C_{Aryl}), 144.0 (C_{Aryl}), 138.5 (C_{Aryl}), 138.0 (C_{Aryl}), 133.2 (C_{Aryl}), 129.2 (C_{Aryl}), 129.0 (C_{Aryl}), 128.9 (C_{Aryl}), 124.8 (C_{Aryl}), 124.7 (C_{Aryl}), 122.5 (C_{Aryl}), 119.3 (C_{Aryl}), 115.2 (C_{Aryl}), 35.4 (C_{Alkyl}), 35.1 (C_{Alkyl}), 31.6 (C_{Alkyl}), 31.5 (C_{Alkyl}), 31.3 (C_{Alkyl}), 25.7 (C_{Alkyl}), 25.6 (C_{Alkyl}), 22.6 (C_{Alkyl}), 16.1 (C_{Alkyl}), 14.1 (C_{Alkyl}). (See Fig. S10†) C,H,N analysis: theoretical $[C_{31}H_{39}N_3]$ = C 82.07 H 8.67, N 9.26; found C 81.22, H 8.49, N 9.19. MS (ESI): *m*/*z* 454.3 $[M + H]^+$.

2-Acetyl-6-{1-[(2,6-dimethyl,4-hydroxyphenyl)imino]ethyl} pyridine (3g). In the crude, the following peaks could be distinguished by ^{1}H NMR (400 MHz, $CDCl_3$; *δ*, ppm) 8.54 (d, 1H, py_m–H), 8.13 (d, 1H, py_m–H), 7.93 (t, 1H, py_p–H), 6.58 (s, 2H, Ph_m–H), 2.79 (s, 3H, O=C(CH_3)), 2.24 (s, 3H, N=C(CH_3)), 1.99 (s, 6H, Ph_m–CH_3), *Ph–OH was not observed in the crude.* ***2,6-Bis{1-[(2,6-dimethyl,4-hydroxyphenyl)imino]ethyl}pyridine (4g)*:** ^{1}H NMR (400 MHz, $(CD_3)_2CO$; *δ*, ppm) 8.53 (d, 2H, py_m–H), 8.09 (t, 1H, py_p–H), 7.83 (s, 2H, Ph_p–OH), 6.66 (s, 4H, Ph_m–H), 2.28 (s, 6H, N=C(CH_3)), 2.00 (s, 12H, Ph_o–CH_3). $^{13}C\{^1H\}$ NMR (100 MHz, $(CD_3)_2CO$; *δ*, ppm) 169.2 (C_q), 157.1 (C_q), 154.7 (C_q), 143.1 (C_q), 138.6 (C_q), 127.8 (Ar–CH), 123.5 (Ar–CH), 116.2 (Ar–CH), 18.9 (Ar–$\mathbf{C}H_3$), 17.3 (N=C($\mathbf{C}H_3$)). (See Fig. S11†) MS (ESI): *m*/*z* 402.2 $[M + H]^+$.

2-Acetyl-6-{1-[(4-methoxyphenyl)imino]ethyl}pyridine (3h). In the crude, the following peaks could be distinguished by ^{1}H NMR (400 MHz, $CDCl_3$; *δ*, ppm) 8.46 (d, 1H, py_m–H), 8.10 (d, 1H, py_m–H), 7.91 (t, 1H, py_p–H) 2.78 (s, 3H, O=C(CH_3)), 2.32 (s, 3H, N=C(CH_3)). ***2,6-Bis{1-[(4-methoxyphenyl)imino]ethyl} pyridine (4h)*:** ^{1}H NMR (400 MHz, $CDCl_3$; *δ*, ppm) 8.33 (d, 2H, py_m–H), 7.85 (t, 1H, py_p–H), 6.96–6.81 (m, 8H, Ph–H), 3.84 (s, 6H, O–CH_3), 2.44 (s, 6H, N=C(CH_3)). *Due to fluxionality in solution/multiple orientations of the imino-aryl/phenoxy groups, a higher number of peaks in the ^{13}C are observed than would be expected for a symmetrical ligand, the ranges are consistent with literature reports*:[38] $^{13}C\{^1H\}$ NMR (100 MHz, $CDCl_3$; *δ*, ppm) 167.5 (C_{Aryl}), 166.7 (C_{Aryl}), 156.5 (C_{Aryl}), 156.2 (C_{Aryl}), 152.8 (C_{Aryl}), 152.7 (C_{Aryl}), 152.3 (C_{Aryl}), 144.1 (C_{Aryl}), 139.8 (C_{Aryl}), 137.9 (C_{Aryl}), 137.1 (C_{Aryl}), 124.8 (C_{Aryl}), 124.7 (C_{Aryl}), 122.3 (C_{Aryl}), 120.1 (C_{Aryl}), 116.5 (C_{Aryl}), 114.8 (C_{Aryl}), 114.2 (C_{Aryl}), 55.9 (O–$\mathbf{C}H_3$), 55.5 (O–$\mathbf{C}H_3$), 25.7 (C_{Alkyl}), 25.5 (C_{Alkyl}), 16.3 (C_{Alkyl}), 16.1 (C_{Alkyl}). (See Fig. S12†). MS (ESI): *m*/*z* 374.2 $[M + H]^+$.

No reaction was observed for ***1*** *and* ***2i*** *(see Fig. S13†).*

General procedure for the scaled-up mechanochemical reaction of 1 with 2a or 2h

In a tungsten carbide vessel, diacetylpyridine **1** 0.006 mol (1.0 g) was mixed with 0.0182 mol (2.20 g) 2,6-dimethylaniline **2a**, or 0.0182 mol (2.24 g) of *p*-methoxyaniline **2h**, 45 mg of *p*-toluenesulfonic acid monohydrate (TsOH), and 700 mg $MgSO_4$ with (2) 11.2 mm WC balls. The reaction vessel was sealed and placed on a SPEX® 8000 mill and allowed to react for 4 h. When complete, an aliquot of the powder/slurry was taken, dissolved in ~0.8 mL $CDCl_3$, and passed through a 0.2 μm PTFE syringe filter. The sample was measured by ^{1}H NMR spectroscopy, and the % composition was determined by the integration of the well-resolved pyridine *meta*-CH peaks (Fig. S1 and S13†). **2a** and **2h** were isolated by the same protocol as described for the smaller scale reactions (*vide supra*).

Synthesis of 2-{1-[(2,4,6-trimethylphenyl)imino]ethyl},6-{1-[(2,6-dimethylphenyl)imino]ethyl}pyridine (4ab). In a steel

vial, 2-acetyl-6-{1-[(2,6-dimethylphenyl)imino]ethyl}pyridine (**3a**) 0.56 mmol (150 mg) was mixed with 0.67 mmol of aniline **2b**, 7 mg of *p*-toluenesulfonic acid monohydrate (TsOH), and 70 mg $MgSO_4$ with (4) 3.175 mm 440c stainless steel balls. The reaction vessel was sealed, and placed on a SPEX® 5100 mill and allowed to react for 4 hours. When complete the reaction was run through a Teledyne ISCO Combiflash® as an elution mixture of ethyl acetate and hexanes. For one minute, the column was flushed with pure hexanes, followed by a gradual ramp from 0% ethyl acetate to 5% ethyl acetate over the course of 1 min. Then, at the start of the second min the percentage of ethyl acetate was ramped from 5% to 15% over a period of 7 min. **4ab** was isolated, concentrated *in vacuo*, and recrystallized from methanol. A fine yellow powder identified as **4ab** was isolated in good yield (152 mg/71%). The reaction could also be run starting with 2-acetyl-6-{1-[(2,4,6-trimethylphenyl) imino]ethyl}pyridine (**3b**) 0.27 mmol (75 mg), 0.32 mmol **2a**, 7 mg of *p*-toluenesulfonic acid monohydrate (TsOH), and 70 mg $MgSO_4$ with (4) 3.175 mm 440c stainless steel balls. After workup, the resulting yield of **4ab** was lower (64 mg/62%) due to smaller reaction size/mechanical loss of product. *Peaks observed in ^1H and ^{13}C are broadened due to ligand asymmetry/fluxionality in solution.* ^{1}H NMR (400 MHz, $CDCl_3$; δ, ppm) 8.49 (brd, 2H, py_m–H), 7.92 (brt, 1H, py_p–H), 7.08 (brd, 2H, Ph_m–H), 6.95 (brt, 1H, Ph_p–H), 6.90 (brs, 2H, Ph_m–H), 2.30 (brs, 3H, Ph_p–CH_3), 2.24 (brs, 6H, N═C(CH_3)), 2.05 (brs, 6H, Ph_o–CH_3), 2.02 (brs, 6H, Ph_o–CH_3). $^{13}C\{^1H\}$ NMR (100 MHz, $CDCl_3$; δ, ppm) 167.5 (C_q), 167.2 (C_q), 155.2 (C_q), 155.1 (C_q), 148.7 (C_q), 137.3 (C_q), 136.8 (C_q), 132.3 (C_q), 128.6 (Ar–CH), 127.9 (Ar–CH), 125.5 (Ar–CH), 125.4 (Ar–CH), 123.1 (Ar–CH), 122.3 (Ar–CH), 20.8 (Ph_p–**C**H_3), 18.0 (Ph_o–**C**H_3), 17.9 (Ph_o–**C**H_3), 16.5 (N═C(**C**H_3)), 16.4 (N═C(**C**H_3)). (See Fig. S16†) C,H,N analysis of a sample recrystallized from methanol was consistent with a 2 : 1 **4ab** : MeOH complex: theoretical $[C_{26}H_{29}N_3]_2[CH_3OH]$ = C 79.66 H 7.82, N 10.52; found C 79.17, H 7.70, N 10.37. MS (ESI): m/z 384.2 $[M + H]^+$. Details for the structure and collection/refinement parameters of single crystals of **4ab** can be found in the ESI.†

Organometallic reactions

Reaction ii: in a WC vial, diacetylpyridine **1** 0.006 mol (1.0 g) was mixed with 0.0182 mol (2.20 g) 2,6-dimethylaniline **2a**, 45 mg of *p*-toluenesulfonic acid monohydrate (TsOH), 0.0055 mol (1.3 g) of $CoCl_2(H_2O)_6$ and 700 mg $MgSO_4$ with (2) 11.2 mm WC balls. The reaction vessel was sealed, and placed on a SPEX® 8000 mill and allowed to react for 4 h. The resulting dark green powder was filtered with DCM (60 mL) to remove $MgSO_4$, concentrated, and rapidly precipitated by the addition of pentane (25 mL) and being held at −24 °C overnight. After drying, 1.87 g of dark green powder was isolated. The product was consistent with {2-acetyl,6{1-[(2,6-dimethylphenyl)imino]ethyl}pyridine}$CoCl_2$ (**6**) as determined by C,H,N analysis: theoretical $[C_{17}H_{18}Cl_2CoN_2O]$ = C 51.54, H 4.58, N 7.07; found C 51.61, H 4.84, N 6.95. This corresponds to a yield of 86%. **Reaction iii:** 150 mg of **6** as synthesized by ***reaction iii*** (*vide supra*) was allowed to stir in a solution of deionized water (3 mL) and pentane (3 mL) for 1 h. The organic portion was extracted, dried, and re-dissolved in 3 mL of methanol, and placed in a freezer at −24 °C overnight. This led to the precipitation of a crystalline yellow powder, which was confirmed to be **3a** by ^{1}H NMR (48 mg, 47% yield).

Conflicts of interest

There are no conflicts to declare.

Acknowledgements

This work was supported by the Department of Chemistry, College of Science, and the FCI at the University of Central Florida. We thank Prof. W. E. Kaden, UCF Physics, for access to a SPEX 8000 mill, Dr. A. Moore (in memoriam) and N. Lapeyrouse, UCF Chemistry, for ESI-MS, Prof. J. Mack, U Cincinnati for kindly supplying the small reaction vial, and Prof. D. S. Richeson, U Ottawa, for helpful discussion.

Notes and references

1 Select examples include: (*a*) I. P. Beletskaya and A. V. Cheprakov, *Chem. Rev.*, 2000, **100**, 3009; (*b*) R. H. Grubbs, *Angew. Chem., Int. Ed.*, 2006, **45**, 3760; (*c*) N. Miyaura and A. Suzuki, *Chem. Rev.*, 1995, **95**, 2457; (*d*) M. Delferro and T. J. Marks, *Chem. Rev.*, 2011, **111**, 2450; (*e*) M. E. van der Boom and D. Milstein, *Chem. Rev.*, 2003, **103**, 1759; (*f*) R. H. Crabtree, *Chem. Rev.*, 1985, **85**, 245.

2 C. M. Zinser, K. G. Warren, R. E. Meadows, F. Nahra, A. M. Al-Majid, A. Barakat, M. S. Islam, S. P. Nolan and C. S. J. Cazin, *Green Chem.*, 2018, **20**, 3246.

3 D. Margetić and V. Štrukil, *Mechanochemical Organic Synthesis*, Elsevier, Cambridge, MA, 2016.

4 (*a*) J.-L. Do and T. Friščić, *ACS Cent. Sci.*, 2017, **3**, 13; (*b*) D. Tan and T. Friščić, *Eur. J. Org. Chem.*, 2018, 18; (*c*) J. Andersen and J. Mack, *Green Chem.*, 2018, **20**, 1435; (*d*) J. L. Howard, Q. Cao and D. L. Browne, *Chem. Sci.*, 2018, **9**, 3080; (*e*) M. Leonardi, M. Villacampa and J. C. Menéndez, *Chem. Sci.*, 2018, **9**, 2042.

5 (*a*) G. N. Hermann, P. Becker and C. Bolm, *Angew. Chem., Int. Ed.*, 2015, **54**, 7414; (*b*) G. N. Hermann, P. Becker and C. Bolm, *Angew. Chem., Int. Ed.*, 2016, **55**, 3781; (*c*) L. Chen, D. Leslie, M. G. Coleman and J. Mack, *Chem. Sci.*, 2018, **9**, 4650; (*d*) R. A. Haley, A. R. Zellner, J. A. Krause, H. Guan and J. Mack, *ACS Sustainable Chem. Eng.*, 2016, **4**, 2464; (*e*) L. Chen, M. O. Bovee, B. E. Lemma, K. S. M. Keithley, S. L. Pilson, M. G. Coleman and J. Mack, *Angew. Chem., Int. Ed.*, 2015, **54**, 11084; (*f*) C. Schumacher, D. E. Crawford, B. Raguž, R. Glaum, S. L. James, C. Bolm and J. G. Hernández, *Chem. Commun.*, 2018, **54**, 8355.

6 N. R. Rightmire and T. P. Hanusa, *Dalton Trans.*, 2016, **45**, 2352.

7 (*a*) J. G. Hernández, I. S. Butler and T. Friščić, *Chem. Sci.*, 2014, **5**, 3576; (*b*) J. G. Hernández, N. A. J. Macdonald, C. Mottillo, I. S. Butler and T. Friščić, *Green Chem.*, 2014, **16**, 1087; (*c*) J.-L. Do, D. Tan and T. Friščić, *Angew. Chem., Int. Ed.*, 2018, **57**, 2667.

8 (*a*) A. Beillard, X. Bantreil, T.-X. Métro, J. Martinez and F. Lamaty, *Green Chem.*, 2018, **20**, 964; (*b*) A. Beillard, T.-X. Métro, X. Bantreil, J. Martinez and F. Lamaty, *Chem. Sci.*, 2017, **8**, 1086.

9 M. Ferguson, N. Giri, X. Huang, D. Apperley and S. L. James, *Green Chem.*, 2014, **16**, 1374.

10 (*a*) N. R. Rightmire, D. L. Bruns, T. P. Hanusa and W. W. Brennessel, *Organometallics*, 2016, **35**, 1698; (*b*) N. R. Rightmire, T. P. Hanusa and A. L. Rheingold, *Organometallics*, 2014, **33**, 5952; (*c*) N. C. Boyde, G. W. Steelman and T. P. Hanusa, *ACS Omega*, 2018, **3**, 8149.

11 (*a*) D. V. Aleksanyan, S. G. Churusova, R. R. Aysin, Z. S. Klemenkova, Y. V. Nelyubina and V. A. Kozlov, *Inorg. Chem. Commun.*, 2017, **76**, 33; (*b*) D. W. Peters and R. G. Blair, *Faraday Discuss.*, 2014, **170**, 83; (*c*) P. Liang, A. Kobayashi, T. Hasegawa, M. Yoshida and M. Kato, *Eur. J. Inorg. Chem.*, 2017, 5134; (*d*) S. A. Kahani and F. Abdevali, *RSC Adv.*, 2016, **6**, 5116; (*e*) V. D. Makhaev, A. P. Borisov and L. A. Petrova, *J. Organomet. Chem.*, 1999, **590**, 222; (*f*) M. Juribašić, K. Užarević, D. Gracin and M. Curić, *Chem. Commun.*, 2014, **33**, 5952; (*g*) J. G. Hernández and C. Bolm, *Chem. Commun.*, 2015, **51**, 12582; (*h*) D. Prochowicz, I. Justyniak, A. Kornowicz, T. Kaczorowski, Z. Kaszkur and J. Lewiński, *Chem. – Eur. J.*, 2012, **18**, 7367; (*i*) J. Lewiński, M. Dutkiewicz, M. Lesiuk, W. Śliwiński, K. Zelga, I. Justyniak and J. Lipkowski, *Angew. Chem., Int. Ed.*, 2010, **49**, 8266; (*j*) D. Prochowicz, I. Justyniak, A. Kornowicz, S. Komorski and J. Lewiński, *Inorg. Chem. Commun.*, 2014, **46**, 216.

12 R. C. Stoufer and D. H. Busch, *J. Am. Chem. Soc.*, 1956, **78**, 6016.

13 E. C. Alyea and P. H. Merrell, *Synth. React. Inorg. Met.-Org. Chem.*, 1974, **4**, 535.

14 (*a*) B. L. Small, M. Brookhart and A. M. A. Bennett, *J. Am. Chem. Soc.*, 1998, **120**, 4049; (*b*) V. C. Gibson, C. Redshaw and G. A. Solan, *Chem. Rev.*, 2007, **107**, 1745; (*c*) G. J. P. Britovsek, V. C. Gibson, S. K. Spitzmesser, K. P. Tellmann, A. J. P. White and D. J. Williams, *J. Chem. Soc., Dalton Trans.*, 2002, 1159.

15 (*a*) C. Bianchini, G. Giambastiani, L. Luconi and A. Meli, *Coord. Chem. Rev.*, 2010, **254**, 431; (*b*) Z. Flisak and W.-H. Sun, *ACS Catal.*, 2015, **5**, 4713; (*c*) T. W. Myers and L. A. Berben, *J. Am. Chem. Soc.*, 2013, **135**, 9988; (*d*) T. Jurca, I. Korobkov, S. I. Gorelsky and D. S. Richeson, *Inorg. Chem.*, 2013, **52**, 5749; (*e*) M. E. Bluhm, C. Folli and M. Döring, *J. Mol. Catal. A: Chem.*, 2004, **212**, 13; (*f*) V. C. Gibson, C. Redshaw, G. A. Solan, A. J. P. White and D. J. Williams, *Organometallics*, 2007, **26**, 5119; (*g*) B. L. Small, M. J. Carney, D. H. Holman, C. E. O'Rourke and J. A. Halfen, *Macromolecules*, 2004, **37**, 4375.

16 (*a*) B. Su, J. Zhao, Q. Zhang and W. Qin, *Polym. Int.*, 2009, **58**, 1051; (*b*) M. Qi, D. Wang and J. A. Byers, *J. Am. Chem. Soc.*, 2018, **140**, 5686.

17 (*a*) M. R. Friedfeld, M. Shevlin, G. W. Margulieux, L.-C. Campeau and P. J. Chirik, *J. Am. Chem. Soc.*, 2016, **138**, 3314; (*b*) B. Raya, S. Biswas and T. V. RajanBabu, *ACS Catal.*, 2016, **6**, 6318.

18 R. Pal, J. A. Laureanti, T. L. Groy, A. K. Jones and R. J. Trovitch, *Chem. Commun.*, 2016, **52**, 11555.

19 T. Jurca, A. Farghal, P.-H. Lin, I. Korobkov, M. Murugesu and D. S. Richeson, *J. Am. Chem. Soc.*, 2011, **133**, 15814.

20 G. M. Duarte, J. D. Braun, P. K. Giesbrecht and D. E. Herbert, *Dalton Trans.*, 2017, **46**, 16439.

21 C. M. Araujo, M. D. Doherty, S. J. Konezny, O. R. Luca, A. Usyatinsky, H. Grade, E. Lobkovsky, G. L. Soloveichik, R. H. Crabtree and V. S. Batista, *Dalton Trans.*, 2012, **41**, 3562.

22 Reaction of **1** with aniline **2g** was improved by the addition of 20 wt% MeOH. However, solvent was not required to initiate reactivity.

23 For the one-pot *two-step* synthesis of salen-type species of Zn, Ni, and Cu, see ref. 9.

24 It was previously reported, on a Diels-Alder system that 4 steel balls leads to the highest yield, similar to herein: K. S. McKissic, J. T. Caruso, R. G. Blair and J. Mack, *Green Chem.*, 2014, **16**, 1628.

25 (*a*) S. M. Hick, C. Griebel and R. G. Blair, *Inorg. Chem.*, 2009, **48**, 2333; (*b*) S. M. Hick, C. Griebel, D. T. Restrepo, J. H. Truitt, E. J. Buker, C. Bylda and R. G. Blair, *Green Chem.*, 2010, **12**, 468.

26 (*a*) G. J. P. Britovsek, M. Bruce, V. C. Gibson, B. S. Kimberley, P. J. Maddox, S. Mastroianni, S. J. McTavish, C. Redshaw, G. A. Solan, S. Strömberg, A. J. P. White and D. J. Williams, *J. Am. Chem. Soc.*, 1999, **121**, 8728; (*b*) B. Raya, S. Jing, V. Balasanthiran and T. V. RajanBabu, *ACS Catal.*, 2017, **7**, 2275.

27 Power consumption monitored on an APC Back-UPS Pro 1500; Spex 5100 mixer mill draws 234 W, comparatively, a standard hotplate stirrer (Thermo Scientific Cimarec+) draws 11 w for stirring at 550 rpm, and peaks at 1.51 kW for heating at 70 °C commensurate with reflux conditions for MeOH.

28 (*a*) E. Peris and R. H. Crabtree, *Chem. Soc. Rev.*, 2018, **47**, 1959; (*b*) M. A. Lawrence, K.-A. Green, P. N. Nelson and S. C. Lorraine, *Polyhedron*, 2018, **143**, 11; (*c*) C. Gunanathan and D. Milstein, *Chem. Rev.*, 2014, **114**, 12024.

29 (*a*) The interaction of C═N with Co results in bond elongation (1643 cm^{-1} ($\nu_{C=N}$), **4a** *vs.* 1598 cm^{-1}, **5**; Fig. S17†), potentially rendering it susceptible to hydrolysis; (*b*) The role of Co in C═N hydrolysis has previously been reported: S. Kumar, S. L. Jain and B. Sain, *RSC Adv.*, 2012, **2**, 789.

30 C. M. Araujo, M. D. Doherty, S. J. Konezny, O. R. Luca, A. Usyatinsky, H. Grade, E. Lobkovsky, G. L. Soloveichik, R. H. Crabtree and V. S. Batista, *Dalton Trans.*, 2012, **41**, 3562.

31 G. R. Fulmer, A. J. M. Miller, N. H. Shreden, H. E. Gottlieb, A. Nudelman, B. M. Stoltz, J. E. Bercaw and K. I. Goldberg, *Organometallics*, 2010, **29**, 2176.
32 C. Görl and H. G. Alt, *J. Mol. Catal. A: Chem.*, 2007, **273**, 118.
33 M. A. Esteruelas, A. M. López, L. Méndez, M. Oliván and E. Oñate, *Organometallics*, 2003, **22**, 395.
34 R. Schmidt, M. B. Welch, R. Knudsen, S. Gottfried and H. G. Alt, *J. Mol. Catal. A: Chem.*, 2004, **222**, 9.
35 F. A. R. Kaul, G. T. Puchta, G. D. Frey, E. Herdtweck and W. A. Herrmann, *Organometallics*, 2007, **26**, 988.
36 M. D. Greenhalgh and S. P. Thomas, *J. Am. Chem. Soc.*, 2012, **134**, 11900.
37 J. Wang, W. Li, B. Jiang and Y. Yang, *J. Appl. Polym. Sci.*, 2009, **113**, 2378.
38 A. L. Vance, N. W. Alcock, J. A. Heppert and D. H. Busch, *Inorg. Chem.*, 1998, **37**, 6912.